www.ijiarec.com

ISSN: 2348-2079

MAR-2015

International Journal of Intellectual Advancements and Research in Engineering Computations

SIMULATION OF SOFT-SWITCHED POWER FACTOR CORRECTION WITH ZVS TWO-SWITCH FORWARD CONVERTER USING MATLAB

S.Vijayakumar

ABSTRACT

A soft-switched continuous-conduction-mode boost power factor correction front-end converter with an integrated zero-voltage-switched two-switch forward second-stage converter is introduced. In the proposed approach, a single transformer is commonly used by the two stages to provide isolation of the power supply and soft switching of all semiconductor switches including a controlled di/dt turn-off rate of the boost rectifier. The performance of the proposed approach was evaluated on a 150-kHz, 430-W/12-V, and universal-line range prototype converter with Mat Lab Software.

Index Terms—Boost converter, magnetic integration, power factor correction (PFC), two-switch forward converter, zero voltage switching (ZVS), Mat Lab Software.

INTRODUCTION

A BOOST power-factor-corrected (PFC) front-end converter followed by a dc-dc two-switch forward converter. This converter combination is off-line power supplies used in low-end computer servers and high-end desktop computers. The front-end boost rectifier is employed to reduce the line-current harmonics and to provide the harmonic limits of the line current in off-line power supplies, whereas the two-switch forward converter is employed to provide galvanic isolation and tight output voltage regulation. The two-switch forward converter topology provides good performance, and low cost. The continuous-conduction-mode (CCM) boost converter is the preferred topology for implementation of a front end with PFC over the range of medium to high power.

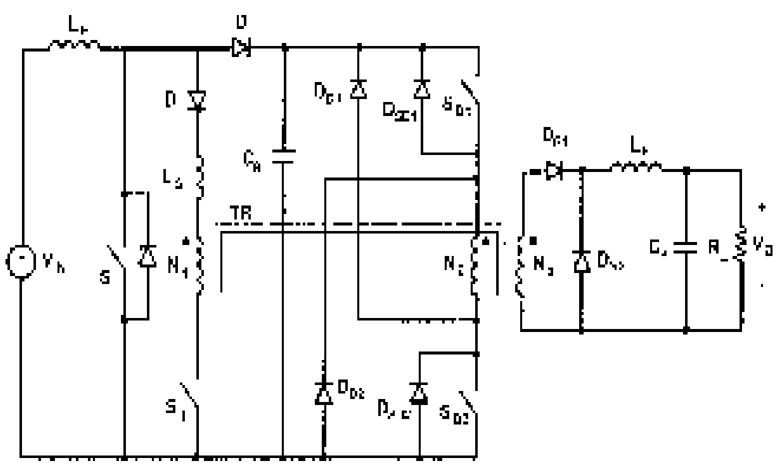

$$v_1 = (N_1/N_3)v_3 = 0.$$

Author for Correspondence:

S.Vijayakumar, Assistant professor, Gnanamani college of Engineering, Namakkal, Tamilnadu, India.
Email:svijaymeped@gmail.com

S.Vijayakumar. et al., Inter. J. Int. Adv. & Res. In Engg. Comp., Vol.–03 (03) 2015 [225-236]

Fig.1. Soft Switched power supply that integrates boost converter and two – switch forward converter

The majority of these developments to reducing the adverse effects of the reverse-recovery characteristic of the boost diode on the conversion efficiency and electromagnetic compatibility (EMC). Similarly, it is optimizing and improving the performance of the two-switch forward converter.

PRINCIPLES OF SOFT-SWITCHED PFC BOOST CONVERTER WITH TWO-SWITCH FORWARD CONVERTER

The proposed soft-switched PFC boost converter with integrated two-switch forward converter is shown in Fig.1. The boost converter consists of voltage source Vin, boost inductor L_B, main switch S, boost rectifier D, energy-storage capacitor C_B, and the active snubber circuit formed by auxiliary switch S_1, winding of transformer TR, snubber inductor L_S, and blocking diode D_1. The two-switch forward converter consists of switches SD_1 and SD_2 associated with antiparallel diodes isolation transformer TR, rectifiers DR_1 and $DR_{2,}$ output inductor $L_{F,}$ and output capacitor $C_{F.}$ To facilitate the explanation of the circuit operation, Fig. 2 shows a simplified circuit diagram of the proposed converter in Fig. 1. In the simplified circuit, energy-storage capacitor C_B is modeled by voltage source by assuming that the value of is large enough voltage ripple, across the capacitor is small in comparison to its dc voltage. In addition, boost inductor L_B and output filter inductor L_F are modeled as constant current sources I_{IN} and I_0, respectively, by assuming that the inductance of L_B and $L_{S.}$ In this analysis, the leakage inductance of the transformer is neglected because it does not have a significant effect. Since snubber inductor L_S and primary winding of transformer TR are connected

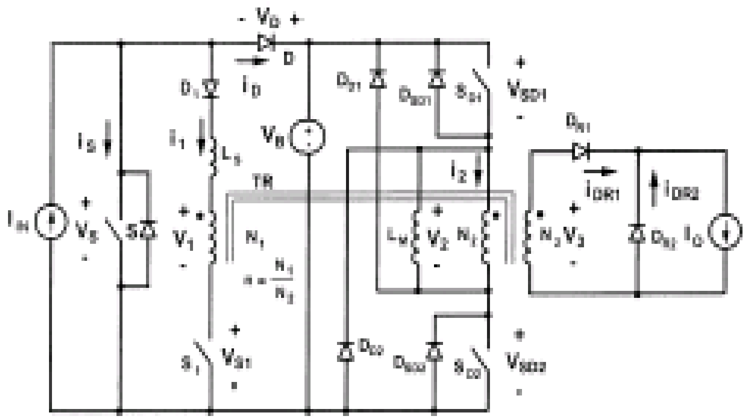

Fig.2. Simplified circuit diagram along with reference of key currents and voltages.

Moreover, by in series, the leakage inductance of the transformer is L_S. As a result, transformer TR is modeled by magnetizing inductance L_M and the three-winding ideal transformer. To further facilitate the analysis of operation, Fig. 3 shows the major topological stages of the circuit in Fig. 1 during a switching cycle, whereas Fig. 4 shows its key waveforms. The reference directions of currents and voltages plotted in Fig. 4 are shown in Fig. 2. As can be seen from the timing diagrams in Fig. 4(a)–(c), the turn on of boost switch S and of forward switches SD_1 and SD_2 and are synchronized, whereas auxiliary switch S_1 is turned on prior to the turn on of switches S, SD_1 and SD2. In addition, auxiliary switch S_1 is turned off before boost switch or forward switches and are turned off. As a result, the entire input current I_{IN} flows through boost rectifier D into energy-storage capacitor C_B in the boost power stage, while output current Io flows through output rectifier DR_2 in the two-switch forward power stage as shown in Fig. 3(j). Because output rectifier DR_2 is conducting during this period, the induced voltage across winding of transformer TR is zero, i.e., $V_1 = (N_1/N_3)$ V3 = 0.

MODES OF OPERATION

STAGE 1

After switch S1 is turned on at t = T_0 the voltage of energy- storage-capacitor C_B is applied across snubber inductor L_S so that current starts to increase linearly, as illustrated in Fig. 4(g). The slope of current is I_L, $d_{i1} / dt = V_B / Ls$ i.e., $IDR_1 = (N_1/N_2) I_1$, as shown in Figs. 3(a) and 4(l). Because output current is constant and equal to the sum of rectifier currents I_{DR1} and I_{DR2}, rectifier current I_{DR2} decreases until it becomes zero when rectifier current I_{DR1} increases. When rectifier current becomes zero at $t = T_1$, output rectifier DR_2 turns off, as shown in Fig. 4(m).

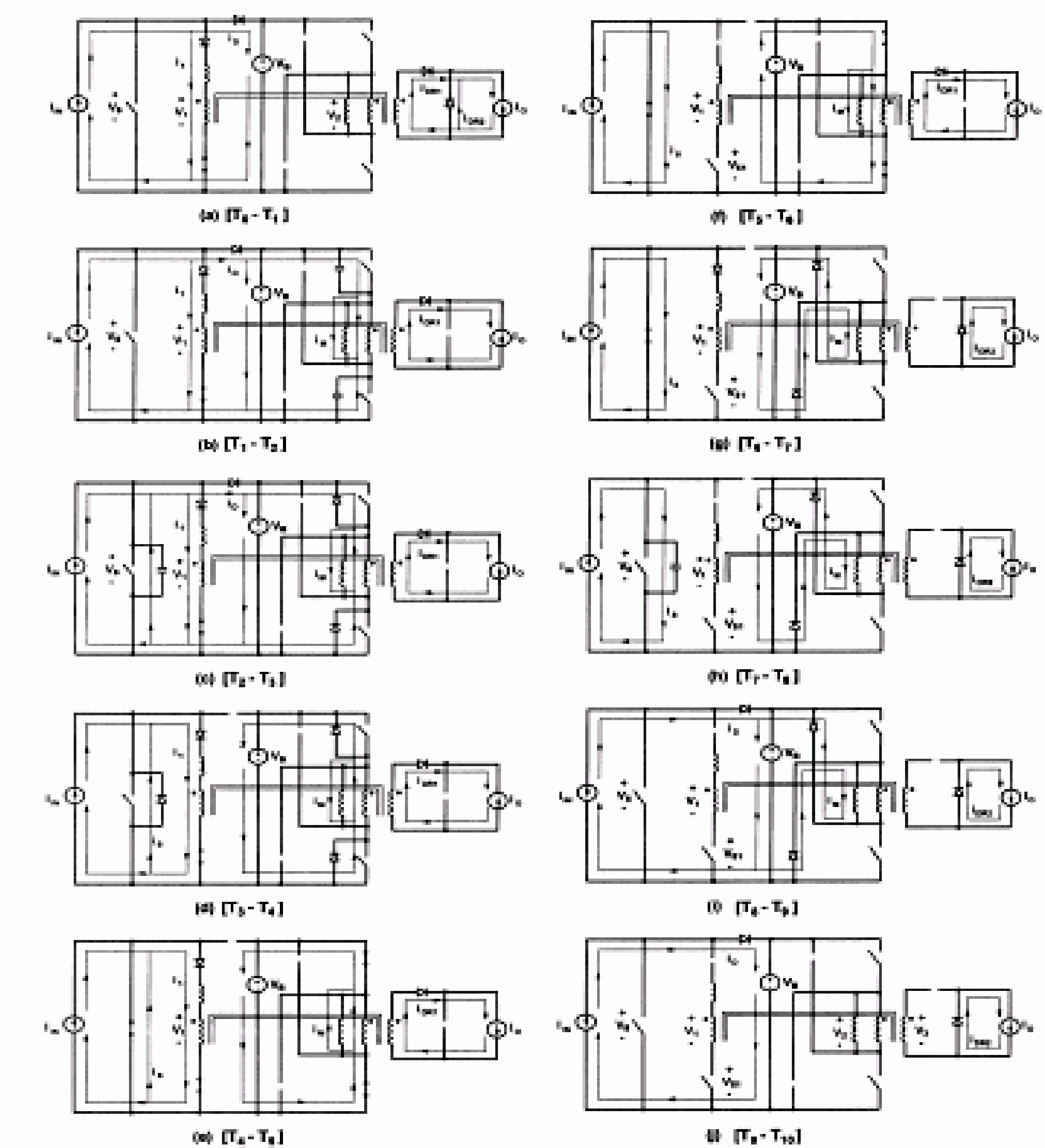

(a) $[T_0 - T_1]$ (f) $[T_5 - T_6]$ (b) $[T_1 - T_2]$ (g) $[T_6 - T_7]$ (c) $[T_2 - T_3]$ (h) $[T_7 - T_8]$ (d) $[T_3 - T_4]$ (i) $[T_8 - T_9]$ (e) $[T_4 - T_5]$ (j) $[T_9 - T_{10}]$

STAGE 2

Since the current through winding N_3 and rectifier DR_1 is equal to output current I_0 after the turn-off of DR_2, the increasing current in winding N_1 makes current I_2 in winding. This current discharges the output capacitances of forward switches SD_1 and SD_2, as illustrated in Figs. 3(b) and 4(i). During this period, voltage V_2 across winding N_2 of transformer TR starts to increase. After the output capacitances of forward switches SD_1 and SD_2 are fully discharged, switch currents ISD_1 and ISD_2 continue to flow through the antiparallel diodes of forward switches and, as shown in Figs. 3(c) and 4(i). To achieve ZVS of forward switches SD_1 and SD_2, While the antiparallel diodes of forward switches SD_1 and SD_2 are conducting, voltage V_2 across winding is equal to V_B, so that induced voltage V_1 on winding N_1 is, $V_1 = N_1/N_2 \times V_B = nV_B$ Because is constant, voltage applied across snubber inductor L_S is also constant so that current I_1 increases linearly with a slope of

Fig. 3 Modes of operation Circuits

During magnetizing inductance increases with a slope given by $d_{iM} / dt = V_B / L$. As current linearly increases, boost rectifier current linearly decreases at the same rate since the sum of and is equal to constant input current. Therefore, in the proposed circuit, the turn-off rate of the boost rectifier $d_{iD} / dt = - (1 – n) V_B/ L_{S,}$

STAGE 3

After t = T_2 current I_1 starts to discharge the output capacitance of boost switch S and charge. The Junction capacitance of boost rectifier D shown in Fig.3(c). If the turns ratio of transformer TR is selected so that n 〈 0.5, the energy stored in is sufficient to completely discharge the output capacitance of boost switch S regardless of the load and line conditions.

STAGE 4

Once the capacitance is fully discharged at t = T_3, current I_S continues to flow through the antiparallel diode of boost switch S, as shown in Figs. 3(d) and 4(h). During this period, voltage V_1 is applied in the negative direction across snubber inductor L_S. Therefore, current I_1 starts to decrease linearly at the rate given by di1/dt = -

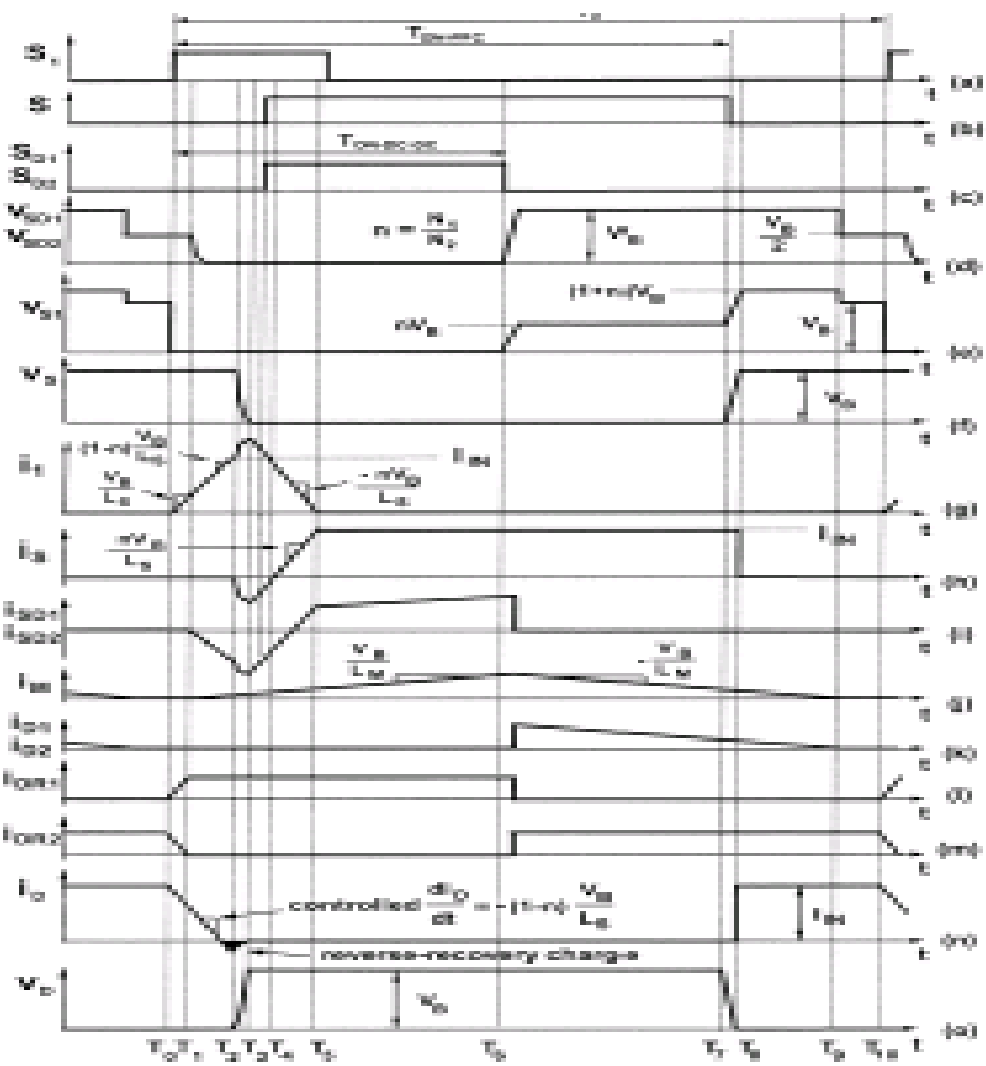

nV_B/L_S, as illustrated in Fig. 4(g). The current in auxiliary switch S_1 also starts to decrease, whereas boost-switch current I_S starts to increase from the negative peak value, as shown in Fig. 4(g) and (h). To achieve ZVS of boost switch S, to turn on boost switch S before its current becomes positive at t = T_4, i.e., during the period when current I_S still flows through the antiparallel diode of switch S, as illustrated in Fig. 4(h). To design the gate signals of the prototype circuit, fixed delay time T_{D1}should be introduced between the turn-on instance of auxiliary S_1 and the turn-on instance of boost switch S. The approximate value of delay time T_{D1} can be calculated by with the condition that turns ratio n is much smaller than 1 and the period between T_1 and T_2 is much shorter than the period between T_0 and T_2. I_{IN} – PEAK is the maximum input current at low line and full load.

$$T_{D1} = \frac{I_{IN} - PEAK}{nV_B/L_S}$$

Fig. 4 Key Waveforms

STAGE 5

In stage 5, after t = T_4, current continues to decrease until it reaches zero at t = T_5, as shown in Fig. 4(g). Shortly after t = T_4, auxiliary switch S_1 is turned off to achieve zero-current switching (ZCS). The gate signal of auxiliary switch S_1 prototype circuit can be a constant on-time pulse signal. Fixed turn-on time T_{ON} – S_1 of auxiliary switch S_1 is approximately given by

$$T_{ON} - S_1 = T_{D1} + \frac{I_{IN} - PEAK}{nV_B/L_S}$$

STAGE 6

After switch S_1 is turned off shortly after t = T_5, the entire input current I_{IN} flows through boost switch. As a result, the front-end boost converter stage is completely decoupled from the two-switch forward converter stage, as shown in Fig. 3(f).

STAGE 7

After forward switches SD_1 and SD_2 are turned off at t = T_6, magnetizing current I_M starts to charge the output capacitances of forward switches SD_1 and SD_2. When voltages V_{SD1} and V_{SD2} reach V_B, the magnetizing current I_M is diverted from forward switches SD_1 and SD_2 to clamp diodes D_{D1} and D_{D2}, as shown in Fig. 3(g). At the same time, bulk voltage V_B applied across winding N_2. During the reset time of the transformer, forward switch voltages V_{SD1} and V_{SD2} are equal to V_0, whereas the voltage across auxiliary switch S_1 is due to the magnetic coupling of winding SN_1 and N_2, as illustrated in Fig. 4(d) and (e).

STAGE 8

After boost switch S is turned off at t = T_7, voltage across switch S starts to increase linearly because constant input current I_{IN} begins charging the output capacitance of boost switch, as shown in Fig. 3(h). The increasing boost-switch voltage causes an equal increase of voltage V_{S1} across auxiliary switch S_1. This stage ends when boost-switch voltage reaches at t = T_8.

STAGE 9

When boost-switch voltage reaches at t = T_8, boost diode D begins to conduct, as shown in Fig. 3(i). At the same time, auxiliary-switch voltage V_{S1} reaches its maximum value of $(1+\prod) V_B$. Until magnetizing current decreases to zero at t = T_9. The next switching cycle is initiated at t = T_{10}. Specifically, boost switch and forward switches and are turned on with ZVS, whereas auxiliary switch is turned off with ZCS. The switch S and forward switches SD_1 and SD_2 are also turned off with soft switching because the output capacitances.

SIMUALTION CIRCUITS AND RESULTS ANALYSIS OF SOFT- SWITCHED PFC WITH ZVS TWO-SWITCH FORWARD CONVERTER USING MATLAB

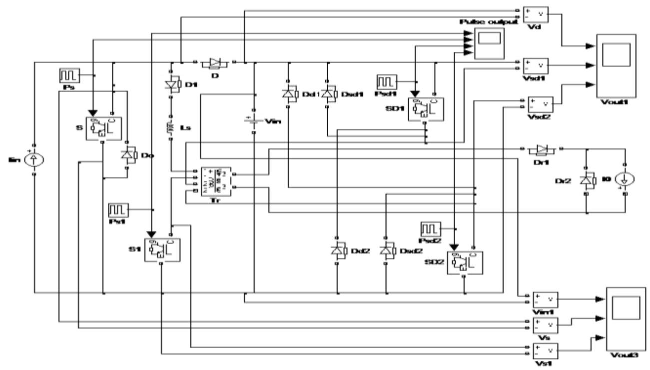

Fig 5.1 Soft Switched power supply that integrates boost converter and two – switch forward converter

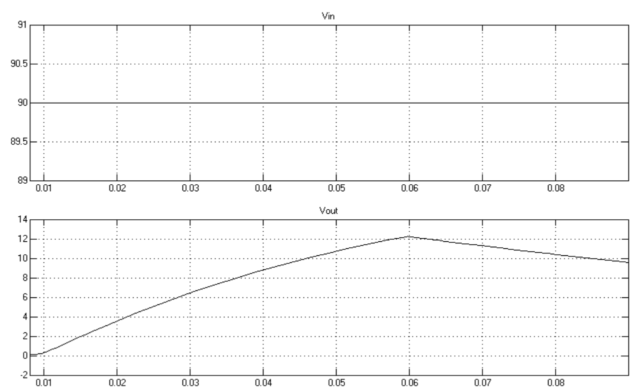

Fig 5.1.1 Input and Output Voltage Wave form

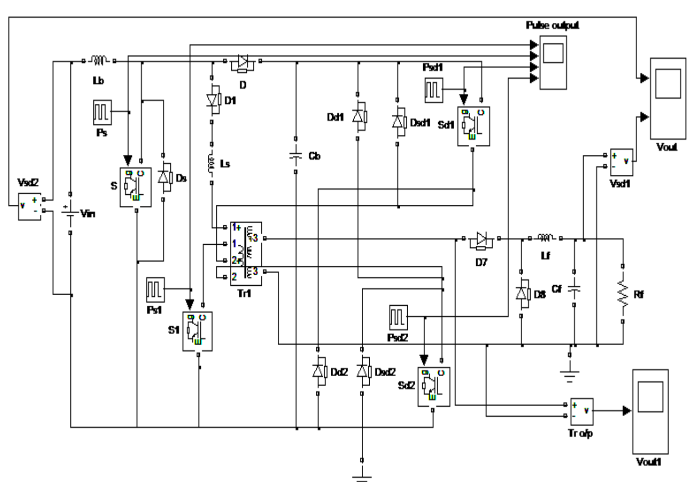

Fig5.2 Simplified Circuit diagram

S.Vijayakumar. et al., Inter. J. Int. Adv. & Res. In Engg. Comp., Vol.–03 (03) 2015 [225-236]

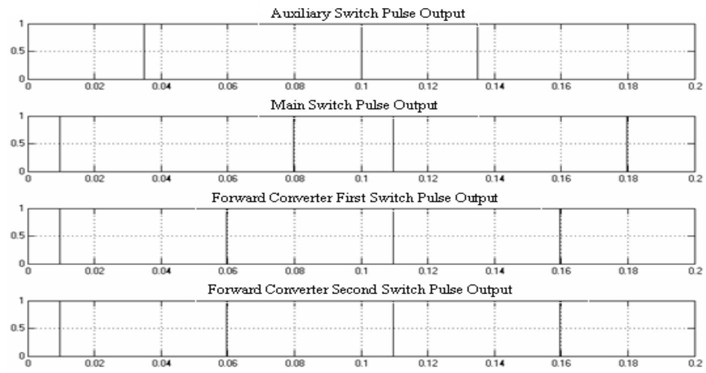

Fig5.2.1 Input Triggering Pulse Wave form

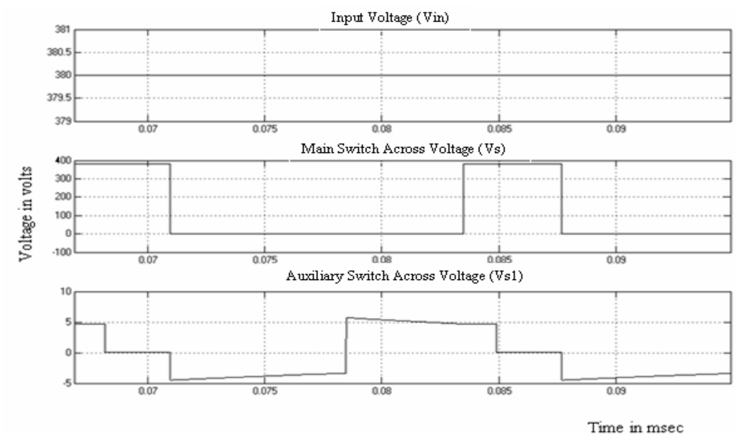

Fig 5.2.2 Wave Form of Vsd1, Vsd2 and V_D

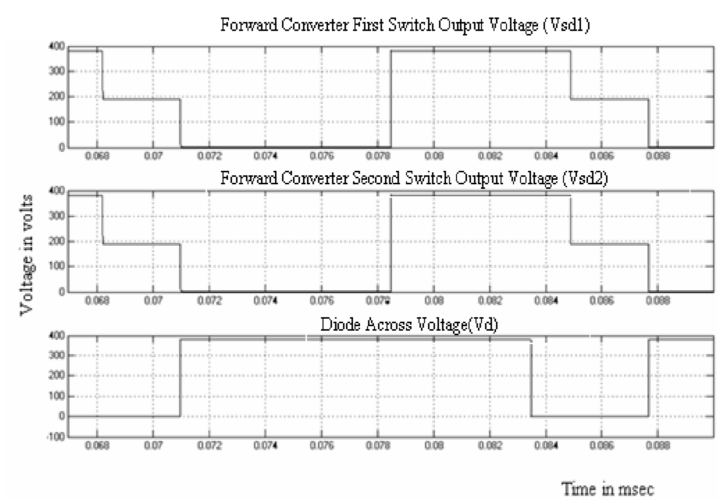

Fig 5.2.3 Wave Form of V_B, Vs and Vs_1

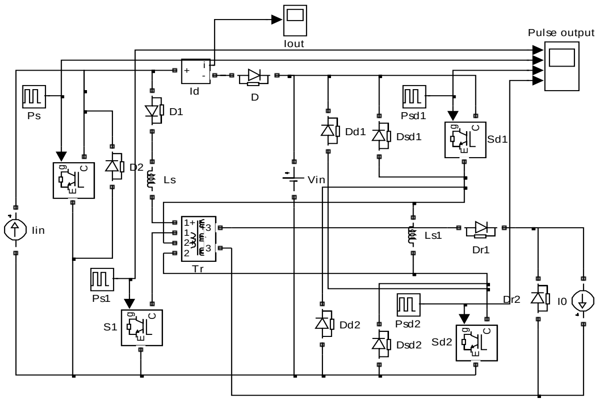

Fig 5.3 Boost Rectifier Current (Id) Circuit

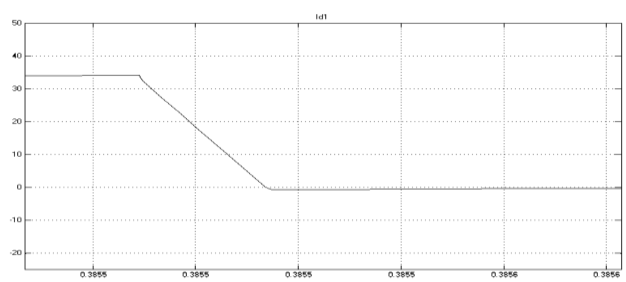

Fig 5.3.1 Boost Rectifier Current (Id) Waveform

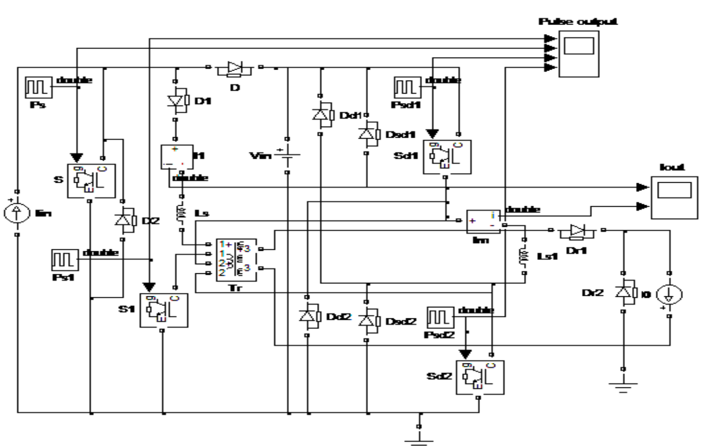

Fig 5.4 Snubber Inductance and Mutual Inductance (I_1 and I_M) Current Circuit

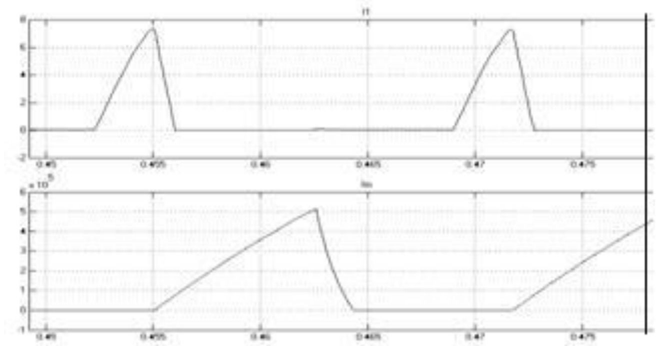

Fig5.4.1 Snubber Inductance and Mutual Inductance (I_1 and I_M) Current Waveforms

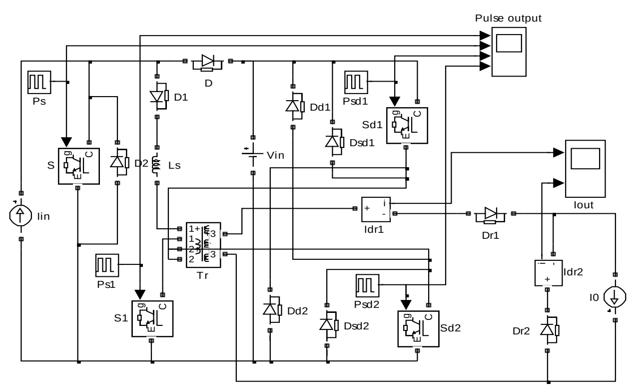

Fig 5.5 Back End Rectifier Current (Idr1and Idr2) Circuit

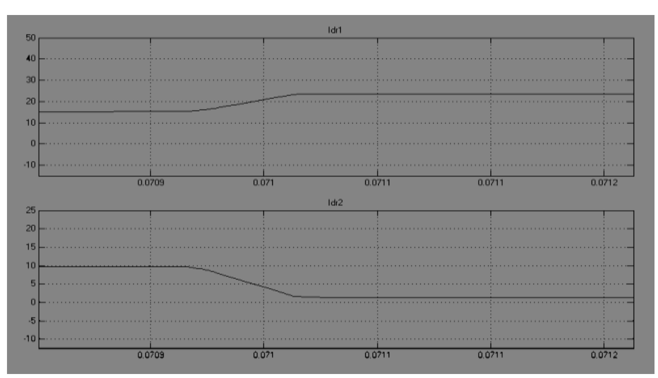

Fig 5.5.1 Back End Rectifier Current (Idr1 and Idr2) Current Waveforms

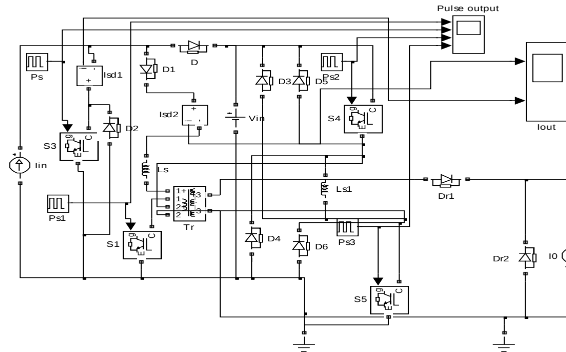

Fig 5.6 Main Switch and Snubber Inductance Current (Is and I_1) Circuit

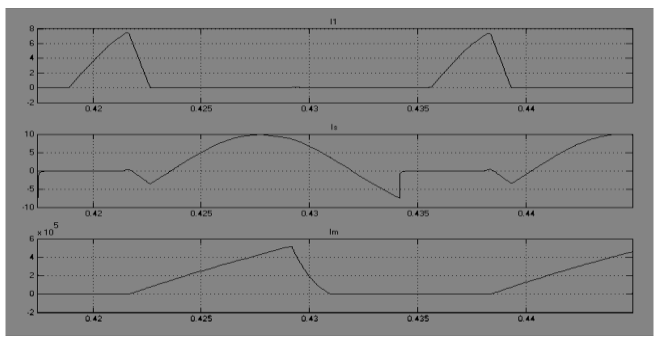

Fig 5.6.1 Main Switch and Snubber Inductance Current (Is and I_1) Current Waveforms

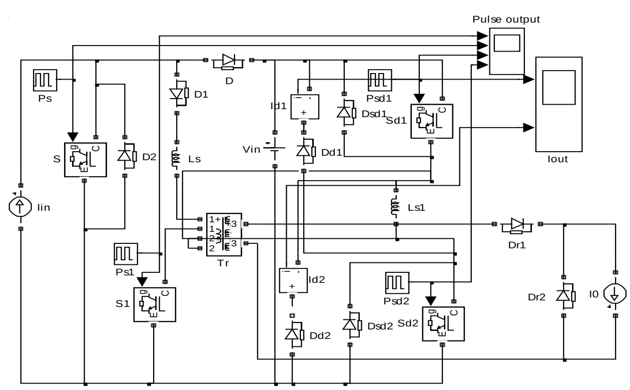

Fig 5.7 Front End Rectifier Current (Id1 and Id2) Circuit

S.Vijayakumar. et al., Inter. J. Int. Adv. & Res. In Engg. Comp., Vol.–03 (03) 2015 [225-236]

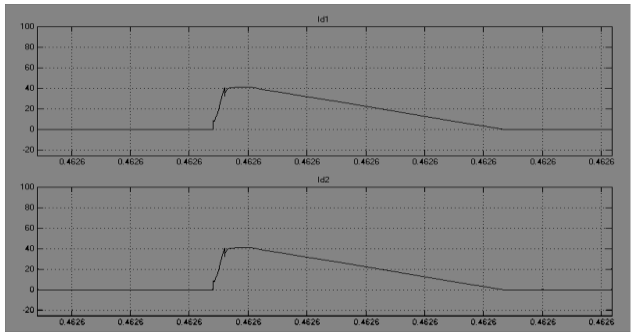

Fig 5.7.1.Front End Rectifier Current (Id1 and Id2) Circuit

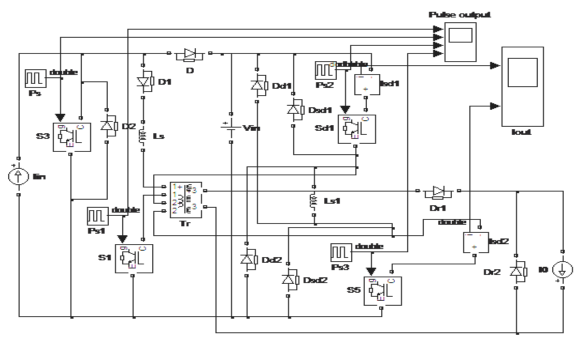

Fig 5.8 Forward Switching Diode Current (Isd1 and Isd2) Circuit

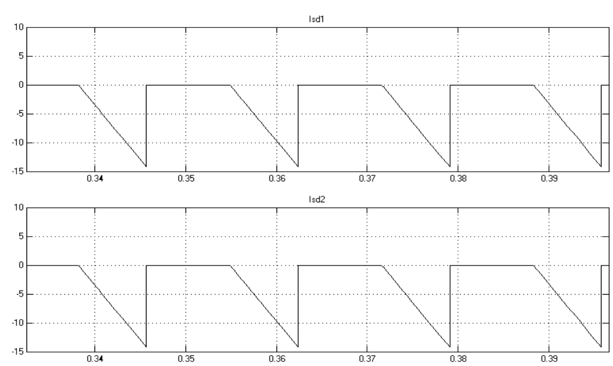

Fig 5.8.1 Forward Switching Diode Current (Isd1 and Isd2) Circuit

CONCLUSION

A soft-switched boost PFC front-end converter with an integrated ZVS two-switch forward second-stage converter has been introduced. By using a single magnetic device which is mutually shared by the PFC boost converter and the two-switch forward Converter, boost switch S and forward switches SD_1 and SD_2 are turned on with ZVS, auxiliary switch S_1 is turned off with ZCS, and boost diode is turned off softly using a controlled rate. As a result, the turn-on switching losses in the boost and forward switches, the turn-off switching loss in the auxiliary switch S_1, and reverse-recovery-related losses in the boost diode D are eliminated, which maximizes the conversion efficiency. The performance of the proposed approach was evaluated on a 150-kHz, 430-W, and universal-line range prototype converter delivering 12-V/36-A output.

REFERENCES

[1]. D. C. Martins, F. J. M. de Seixas, J. A. Brilhante, and I. Barbi, "A family of dc-to-dc PWM converters using a new ZVS commutation cell," in *Proc. IEEE Power Electron. Spec. Conf. (PESC)*, Jun. 1993, pp. 524–530.

[2]. G. Moschopoulos, P. Jain, and G. Joós, "A novel zero-voltage switched PWM boost converter," in *Proc. IEEE Power Electron. Spec. Conf.(PESC)*, 1995, pp. 694–700.

[3]. J.-H. Kim, D. Y. Lee, H. S. Choi, and B. H. Cho, "High performance boost PFP (power factor pre-regulator) with an improved ZVT (zero voltage transition) converter," in *Proc. IEEE Appl. Power Electron.(APEC) Conf.*, 2001, pp. 337–342.

[4]. F. T. Wakabayashi, M. J. Bonato, and C. A. Canesin, "Novel high power factor ZCS-PWM pre-regulators," *IEEE Trans. Ind. Electron*, vol. 48, no. 2, pp. 322–333, Apr. 2001.

[5]. H. S. Choi and B. H. Cho, "Zero-current-switching (ZCS) power factor pre-regulator (PFP) with reduced conduction losses," in *Proc. IEEE Appl. Power Electron. (APEC) Conf.*, 2002, pp. 962–967.

[6]. H. Chung, S. Y. R. Hui, and K. K. Tse, "Reduction of power converter EMI emission using soft-switching technique," *IEEE Trans. Electromagn.Compat.*, vol. 40, no. 3, pp. 282–287, Aug. 1998. [7] A. P. Patel, "Forward Converter Circuit Having Reduced Switching Losses," U.S. Patent 6 370 051B1, Apr. 9, 2002.

[7]. G. Huang, Y. Gu, Z. Liu, and A. J. Zhang, "Resonant Reset Dual Switch.

[8]. High – Power – Factor –Correction Soft SwitchedBoost Converter Yungtack jang, senior Member , IEEE,Milon M.Jovanovic, Fellow, IEEE, Kung – Hui-fung, and Yu - Ming chang.